Journal of Medicinal Chemistry

Article

Cite This: J. Med. Chem. 2017, 60, 8731-8740

pubs.acs.org/jmc

Structural Basis of Inhibition of ERα-Coactivator Interaction by High-Affinity N-Terminus Isoaspartic Acid Tethered Helical Peptides

Mingsheng Xie,[†] Hui Zhao,[†] Qisong Liu,[‡] Yujia Zhu,[§] Feng Yin,[†] Yujie Liang,[†] Yanhong Jiang,[†] Dongyuan Wang,[†] Kuan Hu,[†] Xuan Qin,[†] Zichen Wang,[∥] Yujie Wu,[▽] Naihan Xu,[⊥] Xiyang Ye,[*,#] Tao Wang,[*,▽] and Zigang Li[*,†]

[†]School of Chemical Biology and Biotechnology, Shenzhen Graduate School of Peking University, Shenzhen 518055, China

[‡]Shenzhen Key Lab of Tissue Engineering, The Second People's Hospital of Shenzhen, Shenzhen 518035, China

[§]Department of Radiation Oncology, State Key Laboratory of Oncology in South China, Collaborative Innovation Center for Cancer Medicine, Sun Yat-sen University Cancer Center, Guangzhou 510060, Guangdong, China

[∥]Shenzhen Middle School, Shenzhen 518001, China

[⊥]Key Lab in Healthy Science and Technology, Division of Life Science, Shenzhen Graduate School of Tsinghua University, Shenzhen 518055, China

[#]Department of Gynecology, Shenzhen People's Hospital, Shenzhen 518020, China

[▽]Department of Biology, Southern University of Science and Technology, Shenzhen 518055, China

Supporting Information

ABSTRACT: Direct inhibition of the protein−protein interaction of ERα and its endogenous coactivators with a cell permeable stabilized peptide may offer a novel, promising strategy for combating ERα positive breast cancers. Here, we report the co-crystal structure of a helical peptide stabilized by a N-terminal unnatural cross-linked aspartic acid (**TD**) in complex with the ERα ligand binding domain (LBD). We designed a series of peptides and peptide **6** that showed direct and high-affinity binding to ERα with selective antiproliferative activity in ERα positive breast cancer cells. The co-crystal structure of the **TD**-stabilized peptide **6** in complex with ERα LBD further demonstrates that it forms an α helical conformation and directly binds at the coactivator binding site of ERα. Further studies showed that peptide $\mathbf{6}_{\mathbf{W}}$ could potently inhibit cellular ERα's transcriptional activity. This approach demonstrates the potential of **TD** stabilized peptides to modulate various intracellular protein−protein interactions involved in a range of disorders.

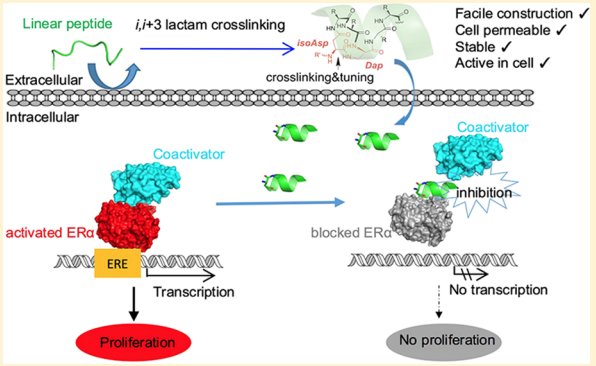

INTRODUCTION

Nuclear receptors (NRs) are multidomain transcription factors that bind to DNA response elements and recruit cofactor proteins to regulate gene transcription.[1] The action of most NRs can be modulated by ligand binding to the binding pocket of the NR ligand binding domains (LBD) that induces subsequent conformational change of the NR determining the interaction with cofactor proteins.[2] The NR superfamily includes the estrogen receptors (ER) ERα and ERβ.[3] ERα is overexpressed in many breast cancer cells and promotes proliferation of estrogen dependent cancer cells.[4] Competitive inhibitors of the ER native ligand 17β-estradiol (E2), such as tamoxifen and raloxifene that target the ligand binding pocket, have been developed as efficient treatments for ERα-positive breast cancers.[5−7] However, drug resistance often emerges after prolonged treatment with these endocrine therapies.[7−9] Recently identified, constitutively active ERα mutants implicated in cancer metastasis highlight the need for identifying new inhibitors that target sites other than the ligand binding pocket of ER for potential therapy to intractable ERα positive breast cancers.[10−13] The transactivation activity of ERα requires the recruitment of coactivator protein such as p160 family coactivator, SRC-1. This interaction is mediated by an α-helical peptide with a conserved LXXLL motif (where L is leucine and X is any amino acid), known as the NR box (nuclear receptor box).[14,15] The short LXXLL sequence is sufficient for binding of ERs and residues adjacent to the core LXXLL motif provide selectivity between the NR superfamily members.[15−18]

Protein−protein interactions (PPIs) with large, shallow, or discontinuous interfaces are generally considered as "undruggable" by traditional small-molecule inhibitors.[19] Stabilized

Received: May 24, 2017
Published: October 18, 2017

DOI: 10.1021/acs.jmedchem.7b00732
J. Med. Chem. 2017, 60, 8731−8740

peptide epitope mimics, which circumvent the poor in vivo stability and membrane permeability of linear peptides, might interrupt PPIs and become promising therapeutics.[20−23] Various synthetic modifications to stabilize peptides into fixed secondary structures (mainly α helices) were developed to disrupt different PPIs.[24−28] Several short stabilized peptide derivatives based on the LXXLL sequence had been reported to disrupt ERα−coactivator interactions in vitro.[29−34] However, only limited cellular activity studies of helically constrained peptides were reported.[35]

Recently, we reported a facile helix-nucleating template based on an unnatural cross-linked aspartic acid at the N-terminus (**TD** strategy) to stabilize peptide into a helical conformation by forming an i, i+3 lactam linkage between isoAsp (L-isoaspartic acid) and Dap (2,3-diaminopropionic acid), leading to improved proteolytic stability and cell penetration.[36] Here, we report the crystal structure of a **TD** stabilized peptide in complex with its target human ERα LBD at 2.4 Å resolution, which is similar to several crystal structures of other helix-stabilized peptides in complex with ERα LBD.[31,33,34] The crystal structure shows the **TD** stabilized peptide folds into a helical conformation and binds at the coactivator binding site of its target, human ERα LBD. We report the synthesis of a pair of highly active and cell-permeable peptide-based ERα inhibitors by combining the peptide side chain cross-linking strategy with peptide surface side chain remodeling. To the best of knowledge, the most potent peptide $\mathbf{6}_\mathbf{W}$ is the first reported **TD** stabilized peptide that efficiently inhibits the proliferation of human ERα positive breast adenocarcinoma cells by targeting cellular ERα-coactivator interaction with IC_{50} of ~12 μM for MCF7 cells and shows little toxicity to ERα negative cancer and normal cell lines. Such peptides may be useful for rational development of further therapeutic agents targeting the important ERα−coactivator interaction site other than the ligand binding pocket of ERα that traditional inhibitors such as tamoxifen do. This also provides a possibility to design peptidomimetics targeting orphan nuclear receptors for which antagonists are difficult to identify.[37]

RESULTS AND DISCUSSION

Crystal Structure of Human ERα LBD in Complex with TD Stabilized Peptide 2. We prepared the linear peptide ligand Ac-Trp-βAla-His-Lys-Ile-Leu-His-Arg-Leu-Leu-Gln-NH_2 based on the sequence of SRC-$Box2_{691-699}$ involved in binding to ERα (here termed peptide $\mathbf{1}_\mathbf{W}$, tryptophan labeled peptide is named followed by a W) and the N-capped peptide $\mathbf{2}_\mathbf{W}$ (Ac-Trp-βAla-Arg-cyclo(isoAsp-Ile-Leu-Dap)-Arg-Leu-Leu-Gln-NH_2) stabilized by the **TD** strategy. The FITC (fluorescein isothiocyanate) labeled cross-linked peptide $\mathbf{2}_{\mathbf{FITC}}$ showed a slightly higher selectivity toward ERα compared to linear $\mathbf{1}_{\mathbf{FITC}}$ among other nuclear receptors such as ERβ and vitamin D receptor in vitro.[36] We initially tested the cellular activities of the linear control peptide $\mathbf{1}_\mathbf{W}$ and cross-linked peptide $\mathbf{2}_\mathbf{W}$ to ERα overexpressed MCF7 cells. The linear ERα peptide ligand $\mathbf{1}_\mathbf{W}$ showed minimal cell killing activity (98.5% viability) in a cell viability assay (Table 1) in which ERα overexpressed MCF7 cells were treated with 20 μM peptide for 24 h. Cross-linked peptide $\mathbf{2}_\mathbf{W}$ showed moderate killing ability (64.5% viability). We also found that $\mathbf{2}_{\mathbf{FITC}}$ showed a slightly higher selectivity to ERα among nuclear receptor progesterone receptors (Figure 1A). To decipher the structural basis of inhibition of the human ERα-coactivator protein interaction with **TD**-stabilized peptide **2**, we overexpressed and purified the

Table 1. Sequences and Biological Activities of the Native and Chemically Modified ER Peptide Ligands

Name	Sequence [a]	Cell viability[b] (%)
1	His-Lys-Ile-Leu-His-Arg-Leu-Leu-Gln	98.5±3.8
2	Arg-cyclo(isoAsp-Ile-Leu-Dap[c])-Arg-Leu-Leu-Gln	64.5±0.4
3	Arg-cyclo(isoAsp-Ile-Leu-Dap)-Arg-Leu-Npg[d]-Gln	43.1±0.8
4	Arg-cyclo(isoAsp-Ile-Leu-Dap)-Arg-Npg-Leu-Gln	53.9±1.1
5	Arg-cyclo(isoAsp-Ile-Npg-Dap)-Arg-Leu-Leu-Gln	53.9±0.4
6	Arg-cyclo(isoAsp-Ile-Npg-Dap)-Arg-Npg-Npg-Gln[e]	14.0±0.2
6*	Arg-cyclo(Dap-Ile-Npg-isoAsp)-Gln-Npg-Arg-Npg	79.2±0.3

[a]All the peptides were amidated at the C-terminus. For the cellular assays, each peptide was labeled with a tryptophan at the N-terminus and acetylated with a βAla linker to determine its concentration by absorption at 280 nm. Ac-Trp-βAla attachment is only for concentration determination and linear peptide **1w** and scramble peptide $\mathbf{6}^*_\mathbf{W}$ with this attachment only show minimal activities in all cellular assays. [b]Cell viability measured with MTT assay by treating ERα overexpressed MCF7 cells (cultured in DMEM supplemented with 10% fetal bovine serum) with 20 μM peptide for 24 h. [c]Dap, 2,3-diaminoprop\ionic acid. [d]Npg, neopentyl glycine. [e]Structure of **6**:

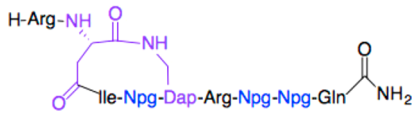

recombinant human ERα ligand binding domain (Supporting Information, Figure S1) and determined the co-crystal structure of peptide **2** with E2 activated ERα LBD at 2.4 Å resolution. The crystal data collection and refinement statistics are shown in Supporting Information, Table S1. As shown in Figure 1B, peptide **2** adopts an amphipathic α-helical conformation where the side chains of Leu4 and Leu8 of **2** are buried in a hydrophobic groove while the side chain of Leu7 of **2** docks into a hydrophobic pocket on the ERα surface where coactivator peptide binds. The additional Ile3 of **2** also appears to form a close contact with the receptor. The charged residues (Lys362 and Glu542) flanking the binding groove on ERα form hydrogen bonds with Ile3, Leu4 and Leu7, and Leu8 of peptide **2**, respectively, further stabilizing the complex. The residues from isoAsp2 to Dap5 of **2** form regular backbone (i, i+4) >C═O···HN< hydrogen bonds with Arg6 to Gln9 of **2**, constraining the **TD** stabilized peptide into an ideal α-helix. The i, i + 3 lactam linkage between isoAsp and Dap further stabilizes the helix. The N-terminal tethered Arg of **2** could engage in additional interactions with ERα, but it is not clear if his interaction takes place because of the poor electron density due to its flexibility at the terminus. The high flexibility of the tethered residue at the N-terminal amino site also suggests that this site could be used for further modifications without an effect on binding. The two XX residues in the LXXLL motif (in this case, Dap and Arg) and the i, i+3 lactam linkage between isoAsp and Dap are oriented away from the groove as expected for an amphiphilic helix. The side chain of Leu4 of **2** is deeply embedded within the groove and forms hydrophobic interactions with the side chains of Ile358, Val376, Leu379,

DOI: 10.1021/acs.jmedchem.7b00732
J. Med. Chem. 2017, 60, 8731−8740

A

	K_D(SEM) [nM] ERα[36]	ERβ[36]	Vitamin D Receptor[36]	Progesterone Receptor	ERβ/ERα	VDR/ERα	PR/ERα
$\mathbf{1}_{FITC}$	118(39)	213(46)	142(68)	82(8)	1.8	1.2	0.7
$\mathbf{2}_{FITC}$	85(17)	270(65)	197(64)	178(106)	3.2	2.3	2.1

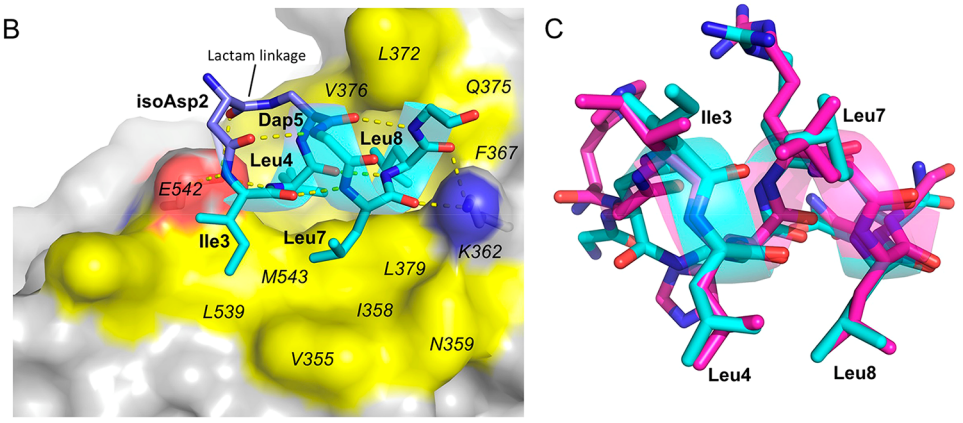

Figure 1. Co-crystal structure of ERα and LBD-**2**(H-Arg-cyclo(isoAsp-Ile-Leu-Dap)-Arg-Leu-Leu-Gln-NH_2) complex (PDB 5GS4). (A) Binding affinity and selectivity of FITC labeled peptides $\mathbf{1}_{FITC}$ and $\mathbf{2}_{FITC}$ to different nuclear receptors. The binding affinity to ERα, ERβ, and vitamin D receptor (VDR) were reported previously.[36] (B) ERα LBD is shown in surface representation, and residues of ERα forming the rim of the binding groove (yellow surface) are labeled in italics. The charged residues Lys362 and Glu542 flanking the binding groove on ERα are labeled blue and red, respectively. Cross-linked peptide **2** (carbon, nitrogen, and oxygen atoms are labeled light blue, blue, and red, respectively) adopts a helical structure, and the side chains of Ile3, Leu4, Leu7, and Leu8 of **2** fill the binding sites in a manner similar to the native ERα peptide ligand. Arg1 and the side chains of other amino acids of **2** are omitted for clarity. The carbon atoms of isoAsp and Dap and the formed lactam linkage are labeled and shown in purple-blue. Lys362 and Glu542 interact with Leu7 and Leu8 and Ile3 and Leu4 of peptide **2**, respectively, by hydrogen bonds (yellow dashed lines), and the main chain hydrogen bonds are also shown in yellow. (C) Comparison of the structures of the bound peptide **2** (blue) with the bound native NR box II peptide (HKILHRLLQ, magenta, PDB 3ERD.) The key hydrophobic residues Ile3, Leu4, Leu7, and Leu8 are labeled.

Glu380, Leu539, Glu542, and Met543 of ERα. The side chain of Leu8 of **2** is also buried into the hydrophobic surface and engages in hydrophobic interactions with the side chains of Ile358, Phe367, Leu372, Gln375, Val376, Leu379, and Lys362 of ERα. The side chain of Leu7 of **2** makes hydrophobic contacts with Val355, Ile358, Lys362, and Asn359 of ERα. Besides, the cross-linked lactam linkage has additional interactions with ERα LBD, which may also contribute to the binding affinity (Figure 1B). The detailed binding patterns are shown in Supporting Information, Figure S4. Superposition of peptide **2**-ERα LBD complex (PDB 5GS4) with NR-box-II peptide (HKILHRLLQDS)-ERα LBD complex (PDB 3ERD[38]) shows **2** binds at the same site on ERα as the linear NR-box-II peptide of coactivator does (root-mean-square derivation of Cα atom is 0.34 Å, Figure 1C, Supporting Information, Figure S4D), indicating that **2** inhibits ERα by directly blocking the interaction between ERα and coactivator proteins.

Design and Synthesis of TD Stabilized ERα Peptide Ligands. Because the linear ERα peptide ligand $\mathbf{1}_W$ showed minimal cellular activity, we modified it and stabilized peptides by the facile **TD** method to improve peptides' cellular activity and synthesized a series of stabilized ERα peptide ligands. Galande et al. reported that the substitution of L^2 of the NR box $L^1XXL^2L^3$ of the disulfide bond stabilized **PERM-2** (H-Arg-cyclo(D-cys-Ile-Leu-Cys)-Arg-Leu-Leu-Gln-NH_2) with its surrogate neopentyl glycine could increase the hydrophobicity of the side chain and might establish additional van der Waals contacts with the isoleucine residue. This could further stabilize the helical conformation of peptide because of the *i*, *i*+4 hydrophobic interaction and improve the binding affinity to ERα.[32] Speltz et al. reported that incorporation of an appropriately positioned γ-methyl group in the side chain of a stapled peptide could increase the helical conformation and binding affinity.[33] However, whether this approach could be applied to the **TD** stabilized peptides to tune the binding affinity to ERα remains unknown. The first crystal structure of **TD** stabilized peptide **2** with ERα LBD in Figure 1B shows that the side chains of Leu4 and Leu8 of **2** are embedded in a hydrophobic groove on the ERα surface with suitable length. On the basis of the crystal structure, we proposed that leucine might be substituted with neopentyl glycine in the **TD** stabilized peptide, which has a side chain with the same length but is slightly bulkier than that of leucine to fill the hydrophobic groove. The substitution of Leu7 to Npg7 might also form hydrophobic interaction with Ile3 of the **TD** cross-linked peptide and further stabilize the peptide's helical conformation to improve its cell penetration ability (Figure 1C). We thus synthesized several analogues of peptide $\mathbf{2}_W$, peptides $\mathbf{3}_W$-$\mathbf{6}^*_W$ and their derivatives, by single- or multipoint substitutions of the LXXLL motif (sequences are shown in Table 1 and Supporting Information, Table S2, representative HPLC data is shown in Supporting Information, Figures S2 and S3) and evaluated their biophysical and biochemical properties and cellular activities.

Circular Dichroism Spectroscopy to Investigate the Helicity of the Peptides. To test the effect of chemical modification on peptide secondary structures, we performed circular dichroism spectroscopy to investigate the solution helicities of the peptides.[39] According to the CD spectra shown in Figure 2, linear peptide $\mathbf{1}_W$ is largely unstructured while peptides $\mathbf{2}_W$–$\mathbf{6}_W$ display helical conformations in ddH_2O. The percent of helicity was calculated as described in experimental

DOI: 10.1021/acs.jmedchem.7b00732
J. Med. Chem. 2017, 60, 8731−8740

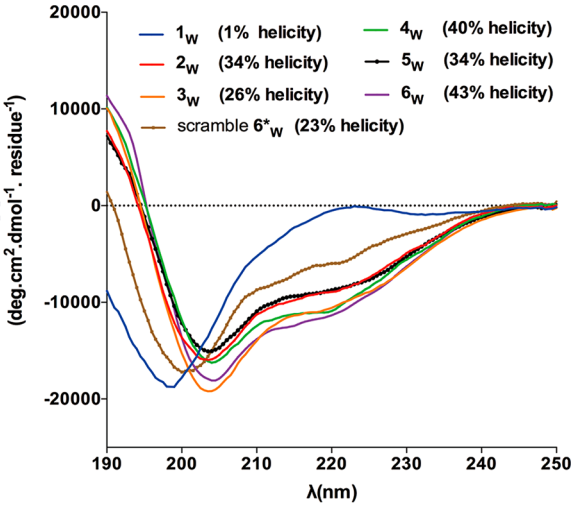

Figure 2. The 190−250 nm region of the CD spectra of peptides at 20 °C in ddH_2O, PH 7.0, and their percent helicities calculated by the $[\theta]_{222}$ value. The linear peptide $\mathbf{1_W}$ is mainly unstructured in ddH_2O, while the stabilized peptides $\mathbf{2_W}$−$\mathbf{6_W}$ show enhanced helical contents.

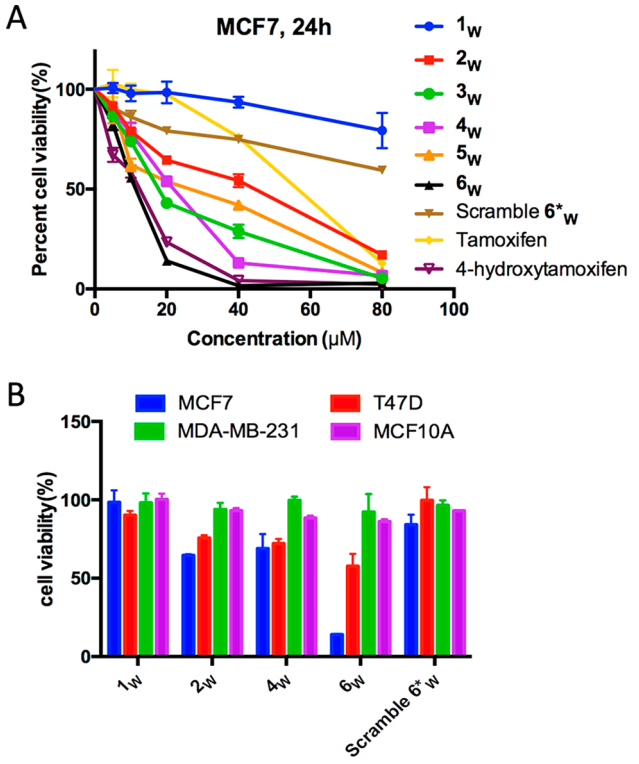

Figure 3. Cellular activities of the peptides. (A) MCF7 viabilities treated by different peptides for 24 h are shown. Tamoxifen and 4-hydroxytamoxifen were used as positive control. (B) The viabilities of ERα positive MCF7, T47D, and ERα negative MDA-MB-231 and normal breast cell line MCF-10A treated by 20 μM different peptides for 24 h are shown.

procedures.[40] $\mathbf{4_W}$ containing a neopentyl glycine at the L^2 position shows increased helicity compared to $\mathbf{2_W}$. We hypothesize that the helical conformation is bolstered by the additional *i*, *i*+4 hydrophobic interactions between the side chains of neopentyl glycine and isoleucine of the amphiphilic peptide. $\mathbf{6_W}$ exhibits the highest helicity (42.9%, Supporting Information, Table S3), suggesting that neopentyl glycine substitutions at L^1 and L^3 positions may form additional *i*, *i*+4 hydrophobic interactions to increase the stabilized peptide's helicity. Peptide $\mathbf{6^*_W}$, with the sequence of $\mathbf{6_W}$ scrambled, showed decreased helicity, suggesting that disruption of the amphiphilic distribution of amino acids on peptide may disfavor its helical conformation.

Cell Killing Ability of the TD Cross-Linked Peptides. The effects of these peptides on the viability of cells were tested by the MTT assay. ERα positive MCF7 cells were incubated with serial dilutions of peptides, and the known ERα inhibitor tamoxifen was used as control. Both the stabilized peptides and tamoxifen showed antiproliferative activity in MCF7 cells, while linear peptide $\mathbf{1_W}$ and scramble $\mathbf{6^*_W}$, which has no binding epitope, showed little toxicity below 20 μM concentration (Figure 3A). Stabilized peptides $\mathbf{3_W}$-$\mathbf{6_W}$ showed higher cell killing ability in a cell viability assay (43.1% to 14.0% viability, Table 1) compared to $\mathbf{2_W}$ (64.5% viability), in which ERα overexpressed MCF7 cells were treated with 20 μM peptide for 24 h. Notably, stabilized peptide $\mathbf{6_W}$ exhibits the most potent dose-dependent inhibition of MCF7 cell viability with an IC_{50} of ∼12 μM. Stabilized peptide $\mathbf{6_W}$ also showed antiproliferative activity to ERα positive T47D breast cancer cells (Supporting Information, Figure S5A). In contrast, the stabilized peptide showed minimal toxicity toward ERα negative MDA-MB-231 cells and the normal breast cells MCF10A (Figure 3B, Supporting Information, Figure S5), demonstrating that stabilized peptide $\mathbf{6_W}$ specifically inhibited ERα overexpressed breast cancer cell viability with high efficiency. Thus, we chose peptide **6** for further studies.

Binding Affinity of the Peptides. The binding affinities of the stabilized peptides were evaluated by fluorescent polarization.[41] The **TD** stabilized peptide $\mathbf{2_{FITC}}$−$\mathbf{6_{FITC}}$ showed high binding affinity to ERα LBD measured by fluorescent polarization. The binding affinities of the representative ER peptide ligands to ERα LBD in the presence of E2 were also verified by isothermal titration calorimetry (ITC) (Figure4, Supporting Information, Figures S6, S7). The ITC data also showed that the binding of ER peptide ligands to ERα LBD required 17β-estradiol (E2) and could be blocked in the presence of ERα inhibitor, 4-hydroxytamoxifen (OHT) (Supporting Information, Figure S6). $\mathbf{6_{FITC}}$ showed increased binding affinity to ERα (K_D = 67(6) nM) in the presence of E2 comparable to linear $\mathbf{1_{FITC}}$ (K_D = 118(39) nM). $\mathbf{6^*_{FITC}}$, with the scrambled sequence of $\mathbf{6_{FITC}}$, showed no binding to ERα (Figure 4).

To test the binding selectivity of the **TD** stabilized peptides to ERα, the binding affinity of the **TD** stabilized peptides to ERβ LBD, progesterone receptor (PR) LBD and vitamin D receptor (VDR) LBD, which also belong to the nuclear receptor superfamily, were also measured by fluorescent polarization assay (Supporting Information, Figure S8−S11). $\mathbf{6_{FITC}}$ showed higher ER subtype selectivity (ERβ/ERα = 4.4, Figure 4B) compared to $\mathbf{1_{FITC}}$ (ERβ/ERα = 1.8, Figure 1A). $\mathbf{6_{FITC}}$ also showed higher selectivity to ERα relative to the progesterone receptor and vitamin D receptor (PR/ERα = 4.3, VDR/ERα > 30, Supporting Information, Table S4, Figures S10, S11). The selectivity of the surface remodeled peptide **6** to ERα may be caused by increased helicity of the **TD** stabilized peptide **6** in an unbound state and the proper orientation of *tert*-butyl substituents of **6** to the ERα surface. This finding is also supported by Arora's recent report that preferred distinct side chain geometries contribute directly to specificity in protein complex formation.[25,42]

DOI: 10.1021/acs.jmedchem.7b00732
J. Med. Chem. 2017, 60, 8731−8740

A

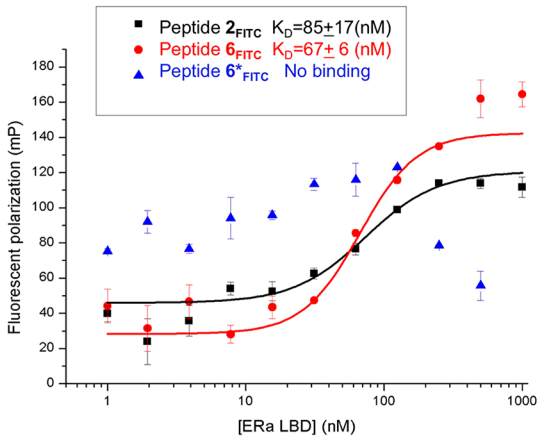

B

	K_D(SEM) [nM] ERα	ERβ	PR	VDR	ERβ/ERα	PR/ERα	VDR/ERα
$\mathbf{6}_{FITC}$	67(6)	297(73)	248(136)	>2000	4.4	3.7	>30

C

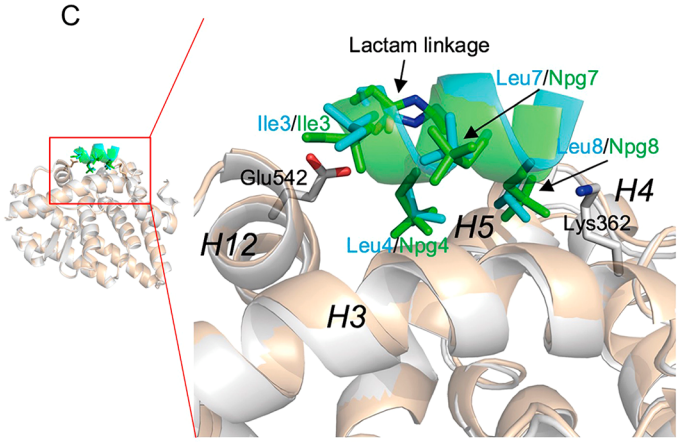

Figure 4. Binding affinity and crystal structure of the most potent peptide **6** with ERα. (A) Fluorescent polarization assay to test the binding affinity of peptide $\mathbf{6}_{FITC}$ with ERα LBD. $\mathbf{2}_{FITC}$ and scrambled $\mathbf{6}^*_{FITC}$ were used as control. (B) Binding affinity of $\mathbf{6}_{FITC}$ to ERα LBD, ERβ, LBD, PR (progesterone receptor) LBD, and VDR LBD. Error bars represent the standard error of mean (SEM) from three independent experiments. (C) Superposition of co-crystal structure of ERα LBD-**6** H-Arg-cyclo(isoAsp-Ile-Npg-Dap)-Arg-Npg-Npg-Gln-NH_2) complex (**6** in green and ERα in wheat, PDB 5GTR) with ERα LBD-**2** complex (**2** in blue and ERα in gray). The lactam linkage and side chains of the key hydrophobic residues are shown as sticks. The helix H3, H4, H5, and H12 of ERα LBD, the lactam linkages and charged residues Lys362 and Glu542 flanking the binding groove on ERα are labeled.

Crystal Structure of ERα LBD in Complex with Peptide 6. To gain a structural understanding of how the most potent peptide **6** binds to ERα, we solved the co-crystal structure of ERα LBD-**6** complex at 2.8 Å resolution. The crystal structure shows that stabilized peptide **6** also binds at the same coactivator binding site formed by helix H3, H4, H5, and H12 of ERα as peptide **2**, with root-mean-square deviation of Cα atoms of 0.50 Å (Figure 4C, Supporting Information, Figure S12). All three neopentyl glycine substitutions of **6** project into the hydrophobic groove at the same site of the E2 activated ERα as respective leucine residues of **2** do with slight shift, while the side chain of Ile3 exhibits a slight rotation. The charged residues Lys362 and Glu542 that flank the binding groove on ERα also further stabilize the binding of **6** to ERα. The residues Dap and Arg and the *i*, *i* + 3 lactam linkage between isoAsp and Dap are oriented away from the groove as expected for an amphiphilic helix. The crystal structure shows that peptide **6** also forms a helical structure, suggesting that the side chains of Ile3 and Npg7, Npg4, and Npg8 at the same face may form hydrophobic interactions to further stabilize the helical conformation of **6** because of their favorable orientations.[32]

Flow Cytometry Analysis to Investigate the Cell Penetration of the Peptides. To test the cytosolic transport of the peptides, we evaluated the cell penetration of the peptides using fluorescence activated cell sorting (FACS). FITC (fluorescein isothiocyanate) labeled, stabilized peptide $\mathbf{2}_{FITC}$ showed improved cell penetration compared to the linear peptide $\mathbf{1}_{FITC}$, while neopentyl glycine substituted **TD** peptide $\mathbf{4}_{FITC}$ and $\mathbf{6}_{FITC}$ showed improved cellular uptake compared to peptides $\mathbf{2}_{FITC}$ and $\mathbf{6}^*_{FITC}$ in MCF7 cells (Figure 5A). This is probably due to their increased helicities which might facilitate cell penetration of the **TD** peptides. Notably, peptide $\mathbf{6}_{FITC}$ shows the highest efficiency in cell penetration although $\mathbf{6}_w$ has similar α-helicity compared to peptide $\mathbf{4}_w$, suggesting that side chain properties may contribute to peptides' cell penetration. On the basis of the crystal structure of bound **6** in Figure 4C, we hypothesize that Ile3 and Npg7 and Npg4 and Npg8 of $\mathbf{6}_{FITC}$ may form hydrophobic interactions to stabilize the helix in the lipid bilayer during membrane penetration because of their favorable *i*, *i*+4 geometry. However, scrambled peptide $\mathbf{6}^*_{FITC}$ showed decreased cell penetration, suggesting that disruption of the helical conformation of peptide influences its cell permeability. The cell penetrating ability of the peptides were also similar in other cell line such as U2OS (Supporting Information, Figure S13), suggesting a similar cell penetration mechanism of the peptides. Additionally, the subcellular distributions of the FITC labeled peptides (green) and ERα (red) were examined using confocal imaging (Figure 5B, Supporting Information, Figure S14).[18] Linear peptide $\mathbf{1}_{FITC}$ showed no cellular uptake, while **TD** stabilized peptide $\mathbf{2}_{FITC}$ and $\mathbf{6}_{FITC}$ showed a diffuse intracellular localization, demonstrating efficient cell penetration. Peptide $\mathbf{6}_{FITC}$ also exhibited increased cell penetration and nucleus accumulation compared to $\mathbf{2}_{FITC}$, which might contribute to its more efficient cellular activities.

RT-PCR to Test the Inhibition Ability of the Peptides to ERα's Transcriptional Activity. The crystal structure of ERα LBD-**6** complex (Figure 4C) shows that stabilized peptide **6** mimics the binding epitope of endogenous coactivators to ERα. To test whether it might disrupt the cellular coactivator–ERα interactions and block the transcriptional activity of ERα, we examined the effect of the peptide on the expression of an endogenous ERα target gene *pS2* in the breast cancer cell line MCF-7 through reverse transcription-quantitative polymerase chain reaction (RT-PCR) analysis.[18] Estrogen deprived MCF-7 cells treated with β-estradiol (E2) showed the expected up-regulation of ERα- mediated *pS2* mRNA levels (normalized to β-actin house-keeping gene mRNA levels, Supporting Information, Figure S15) compared to those without E2

DOI: 10.1021/acs.jmedchem.7b00732
J. Med. Chem. 2017, 60, 8731–8740

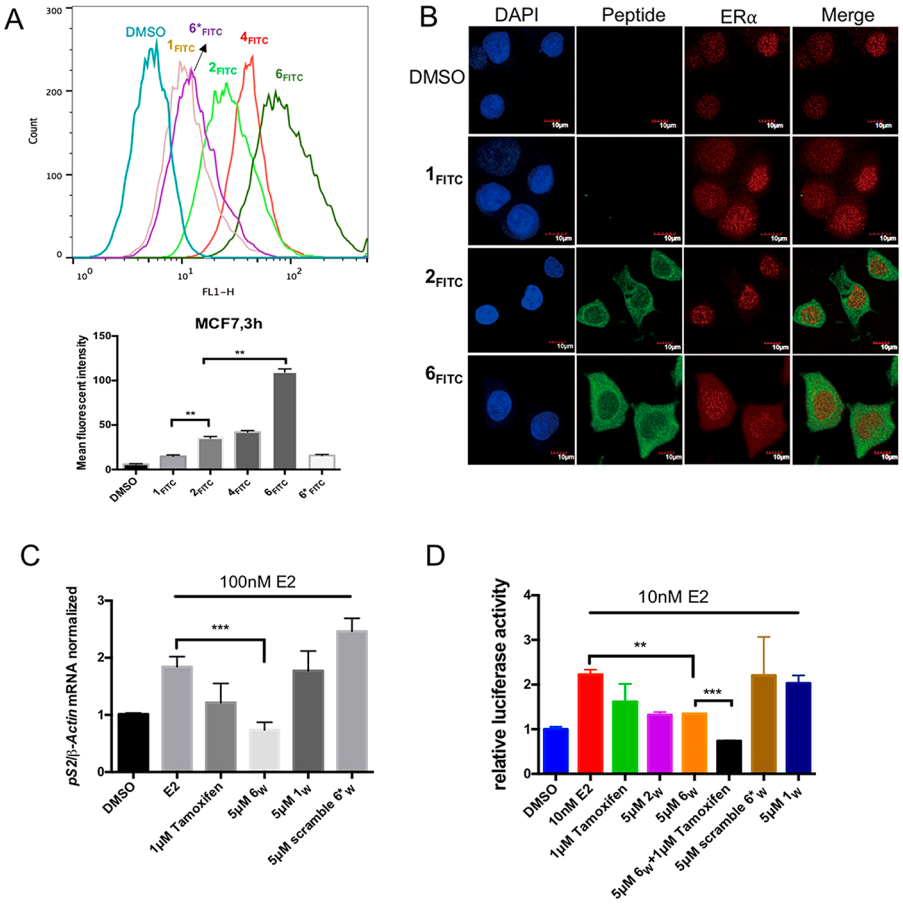

Figure 5. Cell permeability and cellular function of the peptides. (A) FACS analysis to investigate the membrane penetration ability of the FITC labeled peptides. MCF7 cells were treated by 5 μM peptides for 3 h and about 10000 cells were analyzed (top). The mean cellular fluorescent intensity of each analysis was calculated (bottom). Error bars represent for SEM from more than two independent experiments (**P < 0.01 in two-sided Student's t-test). (B) Immunofluorescence and confocal laser scanning microscopy (CLSM) analysis were used to investigate the cellular uptake of peptides $\mathbf{1}_{\mathrm{FITC}}$, $\mathbf{2}_{\mathrm{FITC}}$, and $\mathbf{6}_{\mathrm{FITC}}$ in MCF7 cells. Cells were treated by 5 μM peptides and 10 nM E2 for 3 h. The nucleus was stained by DAPI. The cellular ERα was first immunized by anti-ERα primary antibody and then immunized by Texas-red conjugated goat antirabbit IgG antibody. Scale bar, 10 μm. (C) Effect of stabilized peptides to an endogenous ER-mediated $pS2$ gene's transcription in MCF-7 cells. MCF-7 cells were cultured with indicated peptides in the presence of 100 nM estradiol (E2) or DMSO control. QPCR analysis of endogenous ER-mediated $pS2$ mRNA levels was normalized to β-actin mRNA levels. (D) U2OS cells were cotransfected with pEGFP-C1-ER-α plasmid with 3XERE-Luc ER reporter plasmid which contained the ERE motif for 4 h before treatment with peptides and E2. Luciferase activity was measured using the Dual-Luciferase Assay System. Error bars represent SEM from more than two independent experiments (**P < 0.01, ***P < 0.001 in two-sided Student's t-test).

treatments (Figure 5C). MCF-7 cells treated with E2 and either 1 μM tamoxifen or peptide $\mathbf{6}_{\mathbf{W}}$ (5 μM, which has less than 20% toxicity, Figure 3A) showed significantly decreased $pS2$ mRNA level compared to cells treated by E2 alone, demonstrating the effective down-regulation of the $pS2$ gene expression by the stabilized peptide $\mathbf{6}_{\mathbf{W}}$. In contrast, 5 μM linear peptide $\mathbf{1}_{\mathbf{W}}$ and scrambled $\mathbf{6}^{*}_{\mathbf{W}}$, which had no binding epitope, showed no down regulation of the $pS2$ gene expression.

$\mathbf{6}_{\mathbf{W}}$ Additively Inhibits the Transcriptional Activity of ERα in Combination with Tamoxifen. To further examine whether the stabilized peptide can inhibit ERα transcriptional activity in cells, dual luciferase report assays which test the activity of cellular transcription factors were performed. We co-transfected a plasmid containing a firefly luciferase reporter, gene controlled by 3XEREs (estrogen receptor response elements), into U2OS cells with an expression vector for ERα and a plasmid constitutively expressing pRL-TK *Renilla* luciferase as internal control.[10] The transfected U2OS cells were incubated with or without peptides in the presence of E2, and the reporter gene product was quantified in the resulting cell lysates by measuring the fluorescence generated from the formed oxyluciferin.[18] The relative luciferase activity was first normalized with respect to the constitutive *Rotylenchulus reniformis* luciferase signal and second normalized to the luciferase activity in control cells treated only by DMSO. E2 treatment increased ERα mediated transcription of luciferase gene compared to that without E2 treatment, while tamoxifen and stabilized peptide $\mathbf{6}_{\mathbf{W}}$, but not linear peptide $\mathbf{1}_{\mathbf{W}}$ and scramble $\mathbf{6}^{*}_{\mathbf{W}}$, decreased E2 induced transcription (Figure 5D). Notably, the combination of $\mathbf{6}_{\mathbf{W}}$ and tamoxifen suggested an additive inhibition effect on ERα transcriptional activity. Together, the results suggest that the synthetic **TD** stabilized peptide $\mathbf{6}_{\mathbf{W}}$ could inhibit the ERα–coactivator interaction in cells by targeting ERα, resulting in inhibiting of ERα-mediated gene transcription and the extent of which depends on the amino acid sequences and cell permeability of the peptides.

DOI: 10.1021/acs.jmedchem.7b00732
J. Med. Chem. 2017, 60, 8731−8740

CONCLUSIONS

Breast cancer is the most prevalent cancer in women, and over two-thirds of cases overexpress ERα. Clinical constitutively activated ERα mutants involved in metastases also highlight the need for developing new anti-ERα positive cancer agents. We developed stabilized ERα peptide ligands containing the LXXLL motif analogues by a facile helix-nucleating template based on N-terminal, unnaturally cross-linked aspartic acid (**TD** strategy). We showed, to our best knowledge, for the first time that a facile synthesized **TD** stabilized ERα peptide ligand could potently inhibit the proliferation of ERα positive breast cancer cells with minimal toxicity to normal breast cells. We reported the first co-crystal structure of **TD** stabilized peptide **2** in complex with ERα LBD. The crystal structure of the stabilized peptide helps to reveal the template for designing a series of peptide ligands to disrupt this therapeutically important protein−protein interaction. Among these peptides, **TD** stabilized peptide $\mathbf{6}_{\mathbf{W}}$ exhibited the most potent cellular functions toward ERα positive breast cancer cells by inhibiting cellular ERα−coactivator interaction. The binding affinity (K_D = 67(6) nM) and selectivity of **TD** stabilized peptide $\mathbf{6}_{\mathbf{FITC}}$ to ERα increased compared to the linear ERα peptide ligand $\mathbf{1}_{\mathbf{FITC}}$ among several other nuclear receptors. The selectivity is moderate because the LXXLL motif is shared by many NRs.[43] On the basis of the crystal structure, peptide **6** binds in the coactivator binding groove of ERα instead of the ligand binding pocket, which is targeted by traditional commercial endocrine therapy drugs such as tamoxifen. The slight selectivity may be attributed to the proper geometry of tertiary butyl substituents and the interaction of lactam linkage of **6** with ERα surface. Peptide $\mathbf{6}_{\mathbf{W}}$'s helicity and cellular uptake are significantly improved, leading to its most potent antiproliferation activity to ERα positive MCF7 breast cancer cells. The ERα binding affinity of **TD** peptide $\mathbf{6}_{\mathbf{W}}$ is different from its inhibition potency of cell proliferation, indicating that improving the cell penetrating ability of the ERα peptide ligand may further improve its potency. The cellular activities of **TD** stabilized ERα ligands unambiguously indicated that in addition to enriching the N-cap nucleating peptide stabilization method toolbox, the facile **TD** strategy could be utilized as a reliable way to generate stable and biofunctional peptides. Additionally, the preserved N-terminus NH_2 generated by this **TD** strategy may enable further facile modification for either developing more selective peptides or for drug conjugation. For a proof of concept, the **TD** stabilized peptides show intriguing functions in regulating intracellular ERα−coactivator interactions and have potent cellular activities. The preliminary combination of peptide $\mathbf{6}_{\mathbf{W}}$ and tamoxifen showed additive inhibiting effects in the dual luciferase report assay, hinting that combinatorial treatments using **TD** stabilized peptides with commercial endocrine therapy drugs may be a potentially successful strategy in the clinical setting.

Collectively, these findings may aid in the design of peptidomimetic estrogen receptor modulators in the future and provide insights into the potential clinical translation of these **TD** stabilized peptides. Because of the facile synthesis of **TD** stabilized peptides with all commercially available amino acids and highly efficient, standard on-resin solid phase methods, we expect this strategy to be applicable to the development of a wide array of stabilized peptides to modulate various disordered intracellular protein−protein interactions in diseases such as cancer for therapeutic benefits.

EXPERIMENTAL SECTION

Peptide Synthesis. All reagents and solvents were purchased from Sigma-Aldrich, J&K Co. Ltd., Shanghai Hanhong Chemical Co., GL Biochem (Shanghai) Ltd., and Bide Pharmatech Ltd. and were used without further purification unless otherwise stated. Peptides were synthesized on Rink-amide-MBHA (4-methyl-benzylhydrylamine) resin by Fmoc-based solid phase peptide synthesis (SPPS) as previously reported.[36] Briefly, the Fmoc group was removed by treatment with 50% (v/v) morpholine in NMP (*N*-methyl pyrrolidone) for 30 min × 2. Then the resin was washed sequentially with DCM (dichloromethane) and DMF (dimethylformamide) five times. Fmoc-protected amino acids (5.0 equiv according to initial loading of the resin) and 2-(1*H*-6-chlorobenzotriazol-1-yl)-1,1,3,3-tetramethyluronium hexafluorophosphate (HCTU, 4.9 equiv) were dissolved in DMF and added to resin with coupling reactions by adding *N*,*N*-diisopropylethylamine (DIPEA, 10.0 equiv) with N_2 bubbling for 2 h. The allyl and alloc groups were removed by $Pd(PPh_3)_4$ (0.1eq) and *N*,*N*-dimethylbarbituric acid (4 equiv) in redistilled DCM for two times in the dark, 2 h each time. Cyclization was performed on the resin using benzotriazole-1-yl-oxytripyrrolidino-phosphonium hexafluorophosphate(PyBOP)/1-hydroxybenzotriazole (HOBt)/*N*-methyl morpholine (NMM) (2:2:2.4 equiv) in DMF for two times 5 h. Crude peptides were cleaved from the resins by trifluoroacetic acid (TFA)/ triisopropylsilane (TIS)/H_2O (95:2.5:2.5, v/v) for 2 h. After TFA was removed, crude peptides were precipitated in cold ether. Then ether was removed and crude peptides were dissolved in 20% acetonitrile/H_2O and filtered. FITC labeling was performed on the resin with the solution of FITC (4 equiv) and DIPEA (14 equiv) in DMF in the dark overnight. Crude peptides were further purified by reverse phase-high performance liquid chromatography (RP-HPLC, Shimazu) on a C18-column in acetonitrile/H_2O/TFA, and purity and identity of the products were established by analytic HPLC and mass spectrometry (MS) and were confirmed to have ≥95% purity for all key compounds (Supporting Information, Figure S3, Table S2). FITC labeled peptides were quantified by absorbance of 494 nm with an extinction coefficient of 77000 M^{-1} cm^{-1}. Tryptophan labeled peptides were quantified by absorbance of 280 nm with an extinction coefficient of 5500 M^{-1} cm^{-1}.

Circular Dichroism Spectroscopy (CD). CD spectra were performed at 20 °C using a Chirascan Plus circular dichroism spectrometer. Peptides were dissolved in ddH_2O, pH 7.0, at concentrations of about 100 μM. CD spectra were obtained by wavelengths from 250 to 190 nm with resolution of 0.5 nm, bandwidth of 1 nm, and scanning speed of 20 nm/min. Each spectrum represents the average of two scans with the baseline subtracted and smoothed using Pro-Data Viewer by Applied Photophysics. CD data in ellipticity was converted to mean peptide ellipticity $[\theta]$ in deg·cm^2·$dmol^{-1}$ using the equation $[\theta] = \theta/(10 \times C \times Np \times l)$, where θ is the ellipticity in milidegrees, C is the peptide molar concentration (M), l is the cell path length (cm), and Np is the number of peptide units.[39] Percent helicity was calculated based on the equation described by Arora,[40] helicity % = $[\theta]_{222}/[\theta]\text{max} \times 100$, where $[\theta]\text{max} = (-44000 + 250T)(1 - k/n) = -24818$ for $k = 4.0$ and $n = 11$ (number of amino acid residues in the peptide), T = 20 °C.

Protein Expression and Purification. cDNA encoding human ERα-LBD residues 301−553 was cloned from pEGFP-C1-ER-α plasmid, and cDNA encoding human ERβ LBD residues 259−498 was cloned from pEGFP-C1-ER-β plasmid with mutations C334S, C369S, and C481S. They were then cloned into pET23b via NdeI and *Bam*HI, generating untagged constructs as reported by Phillips et al.[34] Expression was carried out in *Echerichia coli* BL21(DE3) without IPTG induction. Cultures were grown in LB medium at 37 °C to an OD_{600} of about 0.6 before being transferred to 20 °C for another 18 h. Cells were harvested by centrifugation, and the recombinant ERα LBD and ERβ LBD were purified by affinity chromatography. Harvested cells were lysed by sonication in 20 mM Tris-Cl, pH 8.1, 500 mM NaCl, 1 mM EDTA, and 1 mM DTT (buffer A). Cell debris was removed by centrifugation, and the supernatant was loaded on column filled with Estradiol Sepharose 6B Novel Immobilized Steroid Beads (1

DOI: 10.1021/acs.jmedchem.7b00732
J. Med. Chem. 2017, 60, 8731−8740

mL, Polysciences, Inc.) pre-equilibrated by buffer A. After ERα-LBD was carboxymethylated by iodoacetic acid overnight, the column was eluted by 0.1 mM 17β-estradiol (E2) or 0.1 mM 4-hydroxytamoxifen (OHT) in 20 mM Tris, pH 8.1, 0.25 M NaSCN separately and concentrated. The recombinant proteins were further purified by gel filtration using Superdex200 column equilibrated in 50 mM Tris pH 8.1, 150 mM NaCl, and 1 mM TCEP. The SDS-PAGE gel for the purified protein is shown in Supporting Information, Figure S1.

The human vitamin D receptor ligand binding domain (VDR LBD) (residues 156−453) and progesterone receptor (PgR) LBD, comprising residues 678−933, were cloned as a GST fusion protein in pGEX-6p-1 expression vector (GE lifesciences) and overexpressed in *E. coli* BL21 Star (DE3) strain. Cells were grown in LB medium to an OD_{600} of about 0.8 and induced by 0.5 mM IPTG at 289 K for 16 h. The cells were harvested by centrifugation at 5500*g* at 277 K for 20 min. The pellet was washed and resuspended in 50 mL of cold phosphate-buffered saline PBS (140 mM NaCl, 1.8 mM KH_2PO_4, 2.7 mM KCl, 10 mM Na_2HPO_4, pH 7.3). The cells were lysed by sonication on ice. The suspensions were collected by centrifuge at 16000*g* for 1 h at 277 K. The GST fusion protein was purified by GST affinity column and washed with 5 volumes of PBS. Then it was eluted by 10 mM reduced glutathione in 50 mM Tris-HCl (pH 7.3) and further purified by gel filtration. The purified proteins were concentrated by ultrafiltration and stored at −80 °C until use.

Crystallization and Structure Determination. For both the **2**-ERα LBD complex and **6**-ERα LBD complex, the protein containing 17β-estradiol was incubated overnight at 277 K with 2−4-fold molar equivalents of peptide respectively and concentrated to about 5 mg/mL. Crystals of the complex were obtained at 293 K by sitting drop vapor diffusion by mixing 2:1 ratios of protein complex and reservoir solution containing 0.1 M sodium citrate tribasic dihydrate, pH 5.6, 1.0 M and ammonium phosphate monobasic (**2**-ERα LBD complex) or 0.2 M magnesium acetate tetrahydrate and 0.1 M sodium cacodylate trihydrate, pH 6.5, 20% w/v polyethylene glycol 8000 (**6**-ERα LBD complex). Crystals were cryoprotected by transfer to a solution containing 20% glycerol in the mother liquid and flash frozen in liquid nitrogen for use in X-ray diffraction data collection. Data were collected by in house X-ray diffraction system and processed by Crystalclear-2.0 program package (Rigaku) (**2**-ERα LBD complex) or HKL3000 (**6**-ERα LBD complex). Structure was solved by molecule replacement (MR) using 3ERD[38] as a search model. Model building tasks were completed using COOT.[44] Structure refinement was carried out using PHENIX.[45] Data collection and refinement statistics are presented in Supporting Information, Table S1.

Fluorescence Polarization Assay (FP). Fluorescence polarization experiments were performed in 96-well black plates on a plate reader (PerkinElmer, Envision). Briefly, FITC-labeled peptides at a final concentration of 10 nM were mixed with increasing concentration of purified ERα-LBD and ER-β LBD (C334S, C369S, C481S) in assay buffer (10 μM 17β-estradiol, 20 mM Tris-HCl, pH 8.0, 150 mM NaCl, 5% glycerol, and 1 mM TCEP) or GST-VDR LBD (10 μM vitamin D_3, 20 mM Tris-HCl, pH 8.0, 150 mM NaCl, 5% glycerol, and 1 mM TCEP), GST-PgR LBD (10 μM progesterone, 20 mM Tris-HCl pH 8.0, 150 mM NaCl, 5% glycerol, and 1 mM TCEP). The mixtures were then incubated for 40 min in dark. The fluorescence polarizations of the labeled peptides were measured at 298 K using a plate reader (PerkinElmer, Envision) with excitation at 480 nm and emission at 535 nm. The binding affinity (K_D) values were determined by plotting the fluorescence polarization data to concentrations of respectively incubated proteins using nonlinear regression analysis by Origin 7.0 or Prism 6.

Isothermal Titration Calorimetry (ITC). The binding affinities between ERα-LBD and the indicated peptides were also measured using ITC. All experiments were performed with a ITC microcalorimeter (MicroCal iTC200) at 25 °C. For each injection, 2 μL of peptide with a concentration of 50 μM was titrated into 5 μM ERα-LBD in buffer 0.1 mM 17β-estradiol (E2), 50 mM Tris, pH 8.0, 150 mM NaCl, 1 mM TCEP, or 0.1 mM 4-hydroxytamoxifen (OHT), 50 mM Tris, pH 8.0, 150 mM NaCl, 1 mM TCEP in the chamber. The binding data was fitted using the software ORIGIN 7.0.

Cell Viability by MTT Assay. MCF7 and MCF10A were cultured at 37 °C under 5% CO_2 in Dulbecco's Modified Eagle's Medium (DMEM) with phenol red, supplemented with 1% (v/v) antibiotics penicillin/streptomycin (Gibco) and 10% fetal bovine serum (FBS). T47D cells were cultured in RPMI1640 with phenol red, supplemented with 1% (v/v) antibiotics penicillin/streptomycin, 0.2 Units/mL bovine insulin, and 10% FBS. MDA-MB-231 cells were cultured in Leibovitz's L-15 medium without phenol red, supplemented with 10% (v/v) FBS at 37 °C without CO_2. For evaluating cell viability by MTT assay, 100 μL of 5000−10000 cells were seeded each well in the 96-well culture plate and grown in the respective medium overnight. The cells were incubated with serial dilution of peptides, tamoxifen (Sigma), or DMSO control at 37 °C in the medium for 20 h. Then 20 μL of MTT reagent was added and incubated at 37 °C for another 4 h. Then the medium was aspirated, and the formazan product was dissolved in 150 μL of DMSO. The absorbance at 570 nm of dissolved product was measured by a microplate reader (PerkinElmer, Envision).

Flow Cytometry Analysis. Adherent MCF7 or U2OS cells were seeded overnight in 24-well plates and then treated with 5 μM FITC-labeled peptides or DMSO control in FBS-free medium for 3 h at 37 °C. Then supernatant was aspirated, and the plate was wash by PBS, then cells were collected and washed with PBS for three times. The cellular fluorescence intensities of about 10000 cells treated by respective peptide or DMSO control were analyzed each time using a FACS Calibur flow cytometer (BD).

Immunofluorescence and Confocal Microscopy Imaging. MCF7 cells were seeded in 12-well plates on coverslips. The cells were grown overnight in DMEM supplemented with 10% FBS. The cells were then treated with FITC labeled peptide and 10 nM E2 for 3 h at 310 K in the presence of 5% CO_2 followed by washing with PBS for 3 times and fixed in 4% paraformaldehyde in PBS for 15 min at room temperature. For immunofluorescence, after fixation, the cells were treated with 0.25% Triton X-100 for 10 min followed by being blocked in freshly prepared 3% BSA/PBS for 1 h at room temperature and washed by PBS. Then the cells were incubated with rabbit antiestrogen receptor-α antibody (Sigma) at a dilution rate of 1:100 in 3% BSA/PBS solution at 310 K for 1 h. The cells were then washed with PBS and were incubated with Texas red-conjugated goat antirabbit IgG antibody (Santa Cruz) at a dilution rate of 1:300 for 1 h at 310 K. Then coverslips were mounted upside down on slides where previously mounted with medium containing DAPI. Sample cells were imaged using a confocal laser scanning microscope (Olympus) in a dark room, and images acquired were further analyzed by using open source software imageJ.

Quantitative Polymerase Chain Reaction. For quantitative RT-PCR in MCF-7 cells, cells were cultured in phenol red-free DMEM containing 5% charcoal-treated serum (Hyclone) for 72 h in order to deplete activated ER in the cells. Subsequently, cells were treated with indicated peptides or DMSO control for 4 h followed by being treated with 100 nM 17β-estradiol (Sigma) or DMSO control for 16 h. Then cells were washed by PBS, and RNA was extracted using Trizol (TAKARA) according to the manufacturer's protocol. RNA (2 μg) was reverse-transcribed to cDNA using reverse transcriptase kit (Takara), and QPCR was performed using SYBR green (Takara) according to the instructions in a BIORAD real-time PCR system. The *pS2* cDNA was amplified with the forward primer 5′-CATCGA-CGTCCCTCCAGAAGA and the reverse primer 5′-CTCTGG-GACTAATCACCGTGCT as reported.[18] As a control for equal loading, the observed signals were related to β-actin mRNA levels, using a forward primer 5′-CCTGGCACCCAGCACAAT and reverse primer 5′-GGGCCGGACTCGTCATACT. The relative changes in transcript levels for each sample were determined by normalizing to β-actin housekeeping gene mRNA levels. Average values and SEM were obtained from three independent experiments.

Luciferase Reporter Assay. U2OS cells were digested and seeded about 50000 cells per well in 24-well plates and maintained at 37 °C under 5% CO_2 in Dulbecco's Modified Eagle's Medium (DMEM) without phenol red, supplemented with 1% (v/v) antibiotics penicillin/streptomycin and 10% charcoal-stripped fetal bovine

DOI: 10.1021/acs.jmedchem.7b00732
J. Med. Chem. 2017, 60, 8731−8740

serum (hormone-depleted medium) (HyClone). After 1 day, cells were transfected using lipofectame 2000 (Invitrogen) with 200 ng of pEGFP-C1-ER-α plasmid, 200 ng of 3XERE-Luc ER reporter plasmid, and 50 ng of pRL-TK *Renilla* luciferase plasmid (per well) for 4 h before treatment with indicated peptides for 4 h and then treated by E2 (10 nM) or DMSO control for another 20 h. Then the samples were lysed by Passive lysis buffer, and luciferase expression was measured by the Dual-Luciferase Reporter Assay System (Promega). Firefly luciferase activity signal was first normalized with respect to the constitutive *R. reniformis* luciferase signal and second normalized to the luciferase activity in control cells treated by DMSO.

■ ASSOCIATED CONTENT

Supporting Information

The Supporting Information is available free of charge on the ACS Publications website at DOI: 10.1021/acs.jmedchem.7b00732.

SDS-PAGE and gel filtration chromatography, analytical data with RP-HPLC retention times and molecular masses of the synthesized peptides, co-crystal structure of ERα LBD in complex with 17β-estradiol and peptide **2**, cell killing activity of peptides to cell lines T47D, MDA-MB-231, and MCF10A, binding curves of peptides to PgR, ERβ, and VDR ligand binding domain (LBD), and molar elipticities of peptides (PDF)

Molecular formula strings of peptides (CSV)

Crystal structure of ERα LBD in complex with **2**, PDB 5GS4 (PDB)

Crystal structure of ERα LBD in complex with **6**, PDB 5GTR (PDB)

Accession Codes

The crystal structure of ERα LBD in complex with **2** and **6** have been deposited in the Protein Data Bank as entries 5GS4 and 5GTR, respectively. Authors will release the atomic coordinates and experimental data upon article publication.

■ AUTHOR INFORMATION

Corresponding Authors

*For Z.L.: Phone, 0755-26033616; E-mail, lizg@pkusz.edu.cn.
*For X.Y.: E-mail, szyxy2009@hotmail.com.
*For T.W.: E-mail, wangtao@sustc.edu.cn.

ORCID

Yanhong Jiang: 0000-0003-4366-0503
Kuan Hu: 0000-0003-2448-2254
Zigang Li: 0000-0002-3630-8520

Notes

The authors declare no competing financial interest.

■ ACKNOWLEDGMENTS

We thank Dr. Guo Yang and Dr. Liyan Zhou (the Instrument Center of the School of Chemical Biology and Biotechnology in Peking University Shenzhen Graduate School) for help with instrumental analysis. We thank Chuan Shi and Longjian Chen for the preparation of some unnatural amino acids and Prof. Olaf Wiest for helpful discussions. This work is supported by High-Performance Computing Platform of Peking University. We acknowledge financial support from the Natural Science Foundation of China grants 21372023, 21778009, 81701818, 81572198, and 31300600; MOST 2015DFA31590 and 2013CB911501, the Shenzhen Science and Technology Innovation Committee, JCYJ20170412150719814, JCYJ20170412150609690, JCYJ20150403101146313, JCYJ20160301111338144, JCYJ20160331115853521, JSGG20160301095829250, and GJHS20170310093122365; and China Postdoctoral Science Foundation 2017M610704.

■ ABBREVIATIONS USED

ER, estrogen receptor; PR, progesterone receptor; VDR, vitamin D receptor; LBD, ligand binding domain; Fmoc, 9-fluorenylmethoxy-carbonyl; CD, circular dichroism; FITC, fluorescein isothiocyanate; DMF, *N*,*N*-dimethylformamide; TFA, trifluoroacetic acid; DCM, dichloromethane; DIC, *N*,*N*′-diisopropylcarbodiimide; NMM, *N*-methylmorpholine; HCTU, 2-(6-chloro-1*H*-benzotriazole-1-yl)- 1,1,3,3-tetramethylaminium hexafluorophosphate; HOBt, 1-hydroxybenzotriazole; DIPEA, *N*,*N*-diisopropylethylamine; TIS, triisopropylsilane; TFA, trifluoroacetic acid; HPLC, high-performance liquid chromatography; PBS, phosphate buffered saline; EDTA, ethylenediaminetetraacetic acid; DTT, dithiothreitol; GST, glutathione S-transferase; DMEM, Dulbecco'S Modified Eagle Medium; FACS, fluorescence-activated cell sorting; CLSM, confocal laser scanning microscopy; FP, fluorescence polarization; MTT, 3-(4,5-dimethylthiazol-2-yl)-2,5-diphenyltetrazolium bromide; DAPI, 4,6-diamidino-2-phenylindole; RT-PCR, real time polymerase chain reaction; Dap, 2,3-diaminopropionic acid; isoAsp, isoaspartic acid; Npg, neopentyl glycine

■ REFERENCES

(1) Nettles, K. W.; Greene, G. L. Ligand control of coregulator recruitment to nuclear receptors. *Annu. Rev. Physiol.* **2005**, *67*, 309−333.

(2) Darimont, B. D.; Wagner, R. L.; Apriletti, J. W.; Stallcup, M. R.; Kushner, P. J.; Baxter, J. D.; Fletterick, R. J.; Yamamoto, K. R. Structure and specificity of nuclear receptor-coactivator interactions. *Genes Dev.* **1998**, *12* (21), 3343−3356.

(3) Nilsson, S.; Koehler, K. F.; Gustafsson, J. A. Development of subtype-selective oestrogen receptor-based therapeutics. *Nat. Rev. Drug Discovery* **2011**, *10* (10), 778−792.

(4) Holst, F.; Stahl, P. R.; Ruiz, C.; Hellwinkel, O.; Jehan, Z.; Wendland, M.; Lebeau, A.; Terracciano, L.; Al-Kuraya, K.; Janicke, F.; Sauter, G.; Simon, R. Estrogen receptor alpha (ESR1) gene amplification is frequent in breast cancer. *Nat. Genet.* **2007**, *39* (5), 655−660.

(5) Jordan, V. C. Chemoprevention of breast cancer with selective oestrogen-receptor modulators. *Nat. Rev. Cancer* **2007**, *7* (1), 46−53.

(6) Shang, Y.; Brown, M. Molecular determinants for the tissue specificity of SERMs. *Science* **2002**, *295* (5564), 2465−2468.

(7) Peng, J.; Sengupta, S.; Jordan, V. C. Potential of selective estrogen receptor modulators as treatments and preventives of breast cancer. *Anti-Cancer Agents Med. Chem.* **2009**, *9* (5), 481−499.

(8) Musgrove, E. A.; Sutherland, R. L. Biological determinants of endocrine resistance in breast cancer. *Nat. Rev. Cancer* **2009**, *9* (9), 631−643.

(9) Mohseni, M.; Cidado, J.; Croessmann, S.; Cravero, K.; Cimino-Mathews, A.; Wong, H. Y.; Scharpf, R.; Zabransky, D. J.; Abukhdeir, A. M.; Garay, J. P.; Wang, G. M.; Beaver, J. A.; Cochran, R. L.; Blair, B. G.; Rosen, D. M.; Erlanger, B.; Argani, P.; Hurley, P. J.; Lauring, J.; Park, B. H. MACROD2 overexpression mediates estrogen independent growth and tamoxifen resistance in breast cancers. *Proc. Natl. Acad. Sci. U. S. A.* **2014**, *111* (49), 17606−17611.

(10) Toy, W.; Shen, Y.; Won, H.; Green, B.; Sakr, R. A.; Will, M.; Li, Z.; Gala, K.; Fanning, S.; King, T. A.; Hudis, C.; Chen, D.; Taran, T.; Hortobagyi, G.; Greene, G.; Berger, M.; Baselga, J.; Chandarlapaty, S. ESR1 ligand-binding domain mutations in hormone-resistant breast cancer. *Nat. Genet.* **2013**, *45* (12), 1439−1445.

(11) Robinson, D. R.; Wu, Y. M.; Vats, P.; Su, F.; Lonigro, R. J.; Cao, X.; Kalyana-Sundaram, S.; Wang, R.; Ning, Y.; Hodges, L.; Gursky, A.; Siddiqui, J.; Tomlins, S. A.; Roychowdhury, S.; Pienta, K. J.; Kim, S. Y.;

DOI: 10.1021/acs.jmedchem.7b00732
J. Med. Chem. 2017, 60, 8731−8740

Roberts, J. S.; Rae, J. M.; Van Poznak, C. H.; Hayes, D. F.; Chugh, R.; Kunju, L. P.; Talpaz, M.; Schott, A. F.; Chinnaiyan, A. M. Activating ESR1 mutations in hormone-resistant metastatic breast cancer. *Nat. Genet.* **2013**, *45* (12), 1446−1451.
(12) Caboni, L.; Lloyd, D. G. Beyond the ligand-binding pocket: targeting alternate sites in nuclear receptors. *Med. Res. Rev.* **2013**, *33* (5), 1081−1118.
(13) Moore, T. W.; Mayne, C. G.; Katzenellenbogen, J. A. Minireview: Not picking pockets: nuclear receptor alternate-site modulators (NRAMs). *Mol. Endocrinol.* **2010**, *24* (4), 683−695.
(14) Mahajan, M. A.; Samuels, H. H. Nuclear hormone receptor coregulator: role in hormone action, metabolism, growth, and development. *Endocr. Rev.* **2005**, *26* (4), 583−597.
(15) Chang, C.; Norris, J. D.; Gron, H.; Paige, L. A.; Hamilton, P. T.; Kenan, D. J.; Fowlkes, D.; McDonnell, D. P. Dissection of the LXXLL nuclear receptor-coactivator interaction motif using combinatorial peptide libraries: discovery of peptide antagonists of estrogen receptors alpha and beta. *Mol. Cell. Biol.* **1999**, *19* (12), 8226−8239.
(16) Norris, J. D.; Paige, L. A.; Christensen, D. J.; Chang, C. Y.; Huacani, M. R.; Fan, D.; Hamilton, P. T.; Fowlkes, D. M.; McDonnell, D. P. Peptide antagonists of the human estrogen receptor. *Science* **1999**, *285* (5428), 744−746.
(17) Fuchs, S.; Nguyen, H. D.; Phan, T. T. P.; Burton, M. F.; Nieto, L.; de Vries-van Leeuwen, I. J.; Schmidt, A.; Goodarzifard, M.; Agten, S. M.; Rose, R.; Ottmann, C.; Milroy, L. G.; Brunsveld, L. Proline primed helix length as a modulator of the nuclear receptor-coactivator interaction. *J. Am. Chem. Soc.* **2013**, *135* (11), 4364−4371.
(18) Carraz, M.; Zwart, W.; Phan, T.; Michalides, R.; Brunsveld, L. Perturbation of estrogen receptor alpha localization with synthetic nona-arginine LXXLL-peptide coactivator binding inhibitors. *Chem. Biol.* **2009**, *16* (7), 702−711.
(19) Hopkins, A. L.; Groom, C. R. The druggable genome. *Nat. Rev. Drug Discovery* **2002**, *1* (9), 727−730.
(20) Azzarito, V.; Long, K.; Murphy, N. S.; Wilson, A. J. Inhibition of alpha-helix-mediated protein-protein interactions using designed molecules. *Nat. Chem.* **2013**, *5* (3), 161−173.
(21) Milroy, L. G.; Grossmann, T. N.; Hennig, S.; Brunsveld, L.; Ottmann, C. Modulators of protein-protein interactions. *Chem. Rev.* **2014**, *114* (9), 4695−4748.
(22) Milroy, L. G.; Brunsveld, L. Pharmaceutical implications of helix length control in helix-mediated protein-protein interactions. *Future Med. Chem.* **2013**, *5* (18), 2175−2183.
(23) Pelay-Gimeno, M.; Glas, A.; Koch, O.; Grossmann, T. N. Structure-based design of inhibitors of protein-protein interactions: mimicking peptide binding epitopes. *Angew. Chem., Int. Ed.* **2015**, *54* (31), 8896−8927.
(24) Hill, T. A.; Shepherd, N. E.; Diness, F.; Fairlie, D. P. Constraining cyclic peptides to mimic protein structure motifs. *Angew. Chem., Int. Ed.* **2014**, *53* (48), 13020−13041.
(25) Harrison, R. S.; Shepherd, N. E.; Hoang, H. N.; Ruiz-Gomez, G.; Hill, T. A.; Driver, R. W.; Desai, V. S.; Young, P. R.; Abbenante, G.; Fairlie, D. P. Downsizing human, bacterial, and viral proteins to short water-stable alpha helices that maintain biological potency. *Proc. Natl. Acad. Sci. U. S. A.* **2010**, *107* (26), 11686−11691.
(26) Hu, K.; Geng, H.; Zhang, Q.; Liu, Q.; Xie, M.; Sun, C.; Li, W.; Lin, H.; Jiang, F.; Wang, T.; Wu, Y.; Li, Z. An in-tether chiral center modulates the helicity, cell permeability, and target binding affinity of a peptide. *Angew. Chem., Int. Ed.* **2016**, *55* (28), 8013−8017.
(27) Walensky, L. D.; Kung, A. L.; Escher, I.; Malia, T. J.; Barbuto, S.; Wright, R. D.; Wagner, G.; Verdine, G. L.; Korsmeyer, S. J. Activation of apoptosis in vivo by a hydrocarbon-stapled BH3 helix. *Science* **2004**, *305* (5689), 1466−1470.
(28) Tian, Y.; Li, J.; Zhao, H.; Zeng, X.; Wang, D.; Liu, Q.; Niu, X.; Huang, X.; Xu, N.; Li, Z. Stapling of unprotected helical peptides via photo-induced intramolecular thiol-yne hydrothiolation. *Chem. Sci.* **2016**, *7* (5), 3325−3330.
(29) Geistlinger, T. R.; McReynolds, A. C.; Guy, R. K. Ligand-selective inhibition of the interaction of steroid receptor coactivators and estrogen receptor isoforms. *Chem. Biol.* **2004**, *11* (2), 273−281.
(30) Williams, A. B.; Weiser, P. T.; Hanson, R. N.; Gunther, J. R.; Katzenellenbogen, J. A. Synthesis of biphenyl proteomimetics as estrogen receptor-alpha coactivator binding inhibitors. *Org. Lett.* **2009**, *11* (23), 5370−5373.
(31) Leduc, A. M.; Trent, J. O.; Wittliff, J. L.; Bramlett, K. S.; Briggs, S. L.; Chirgadze, N. Y.; Wang, Y.; Burris, T. P.; Spatola, A. F. Helix-stabilized cyclic peptides as selective inhibitors of steroid receptor-coactivator interactions. *Proc. Natl. Acad. Sci. U. S. A.* **2003**, *100* (20), 11273−11278.
(32) Galande, A. K.; Bramlett, K. S.; Trent, J. O.; Burris, T. P.; Wittliff, J. L.; Spatola, A. F. Potent inhibitors of LXXLL-based protein-protein interactions. *ChemBioChem* **2005**, *6* (11), 1991−1998.
(33) Speltz, T. E.; Fanning, S. W.; Mayne, C. G.; Fowler, C.; Tajkhorshid, E.; Greene, G. L.; Moore, T. W. Stapled peptides with gamma-methylated hydrocarbon chains for the estrogen receptor/coactivator interaction. *Angew. Chem., Int. Ed.* **2016**, *55* (13), 4252−4255.
(34) Phillips, C.; Roberts, L. R.; Schade, M.; Bazin, R.; Bent, A.; Davies, N. L.; Moore, R.; Pannifer, A. D.; Pickford, A. R.; Prior, S. H.; Read, C. M.; Scott, A.; Brown, D. G.; Xu, B.; Irving, S. L. Design and structure of stapled peptides binding to estrogen receptors. *J. Am. Chem. Soc.* **2011**, *133* (25), 9696−9699.
(35) Nagakubo, T.; Demizu, Y.; Kanda, Y.; Misawa, T.; Shoda, T.; Okuhira, K.; Sekino, Y.; Naito, M.; Kurihara, M. Development of cell-penetrating R7 fragment-conjugated helical peptides as inhibitors of estrogen receptor-mediated transcription. *Bioconjugate Chem.* **2014**, *25* (11), 1921−1924.
(36) Zhao, H.; Liu, Q.; Geng, H.; Tian, Y.; Cheng, M.; Jiang, Y.; Xie, M.; Niu, X.; Jiang, F.; Zhang, Y.; Lao, Y.; Wu, Y.; Xu, N.; Li, Z. Crosslinked aspartic acids as helix-nucleating templates. *Angew. Chem., Int. Ed.* **2016**, *55* (39), 12088−12093.
(37) Kurebayashi, S.; Nakajima, T.; Kim, S. C.; Chang, C. Y.; McDonnell, D. P.; Renaud, J. P.; Jetten, A. M. Selective LXXLL peptides antagonize transcriptional activation by the retinoid-related orphan receptor RORgamma. *Biochem. Biophys. Res. Commun.* **2004**, *315* (4), 919−927.
(38) Shiau, A. K.; Barstad, D.; Loria, P. M.; Cheng, L.; Kushner, P. J.; Agard, D. A.; Greene, G. L. The structural basis of estrogen receptor/coactivator recognition and the antagonism of this interaction by tamoxifen. *Cell* **1998**, *95* (7), 927−937.
(39) Shepherd, N. E.; Hoang, H. N.; Abbenante, G.; Fairlie, D. P. Single turn peptide alpha helices with exceptional stability in water. *J. Am. Chem. Soc.* **2005**, *127* (9), 2974−2983.
(40) Wang, D.; Chen, K.; Kulp, J. L., III; Arora, P. S. Evaluation of biologically relevant short alpha-helices stabilized by a main-chain hydrogen-bond surrogate. *J. Am. Chem. Soc.* **2006**, *128* (28), 9248−9256.
(41) Vaz, B.; Mocklinghoff, S.; Folkertsma, S.; Lusher, S.; de Vlieg, J.; Brunsveld, L. Computational design, synthesis, and evaluation of miniproteins as androgen receptor coactivator mimics. *Chem. Commun.* **2009**, *36*, 5377−5379.
(42) Watkins, A. M.; Bonneau, R.; Arora, P. S. Side-chain conformational preferences govern protein-protein interactions. *J. Am. Chem. Soc.* **2016**, *138* (33), 10386−10389.
(43) McInerney, E. M.; Rose, D. W.; Flynn, S. E.; Westin, S.; Mullen, T. M.; Krones, A.; Inostroza, J.; Torchia, J.; Nolte, R. T.; Assa-Munt, N.; Milburn, M. V.; Glass, C. K.; Rosenfeld, M. G. Determinants of coactivator LXXLL motif specificity in nuclear receptor transcriptional activation. *Genes Dev.* **1998**, *12* (21), 3357−3368.
(44) Emsley, P.; Cowtan, K. Coot: model-building tools for molecular graphics. *Acta Crystallogr., Sect. D: Biol. Crystallogr.* **2004**, *60*, 2126−2132.
(45) Adams, P. D.; Grosse-Kunstleve, R. W.; Hung, L. W.; Ioerger, T. R.; McCoy, A. J.; Moriarty, N. W.; Read, R. J.; Sacchettini, J. C.; Sauter, N. K.; Terwilliger, T. C. PHENIX: building new software for automated crystallographic structure determination. *Acta Crystallogr., Sect. D: Biol. Crystallogr.* **2002**, *58*, 1948−1954.

DOI: 10.1021/acs.jmedchem.7b00732
J. Med. Chem. 2017, 60, 8731−8740